Impact of R264C and R264H polymorphisms in human aromatase function

Impact of R264C and R264H polymorphisms in human aromatase function

Roberta Baravalle,[1#] Giovanna Di Nardo,[1,2#] Andrea Bandino,[3] Ines Barone,[4] Stefania Catalano,[4] Sebastiano Andò,[4] Gianfranco Gilardi.[1,2,*]

[1] Department of Life Sciences and Systems Biology, University of Torino, via Accademia Albertina 13, 10123 Torino, Italy

[2] CrisDi, Interdepartmental Center for Crystallography, via Pietro Giuria 7, 10125, Torino, Italy

[3] Department of Medicine and Experimental Oncology, University of Torino, Via Michelangelo 27, 10126, Torino, Italy.

[4] Department of Pharmacy, Health and Nutritional Sciences, University of Calabria, Arcavacata di Rende, CS, Italy

[#] These authors contributed equally to the work

Abstract

The cytochrome P450 aromatase is involved in the last step of sex hormones biosynthesis by converting androgens into estrogens. The human enzyme is highly polymorphic and literature data correlate aromatase single nucleotide polymorphisms to the onset of pathologies such as breast cancer and neurodegenerative diseases. The aims of this study were i) to study the influence of the mutations R264C and R264H on the structure-function of the enzyme also upon phospohorylation by selected kinases and ii) to compare the activity of the variants to that of aromatase wild type in two different cell lines.

Far-UV circular dichroism spectroscopy, thermal denaturation experiments and CO-binding assay showed that the two polymorphic variants are correctly folded. Steady-state kinetics experiments showed that rArom R264C and R264H exhibit a 1.5 and 3.4 folds lower catalytic efficiency, respectively, when compared to the wild type protein.

Since R264 is part of the consensus motif of PKA and PKG1, phosphorylation experiments were performed to study the effect on aromatase function. Phosphorylation by PKA caused a decrease in activity by 36.2%, 49.3% and 27.9% in the wild type, R264C and R264H proteins respectively. Phosphorylation by PKG1 was also found to decrease the activity by 30.3%, 30.5% and 15.4% in the wild type, R264C and R264H proteins respectively.

Experiments performed on the three full-length proteins expressed in human MCF-7 breast cancer cells and rat ST14A neuronal cells showed that, depending on the cell line used, the activity of the proteins is different, implicating different cellular mechanisms modulating aromatase activity.

This work demonstrate that R264 polymorphism causes an intrinsic alteration of aromatase activity together with a different consensus for phosphorylation by different kinases, indicating that estrogen production can be different when such mutations are present.

These findings are significant in understanding the onset and treatment of pathologies in which aromatase has been shown to be involved.

Keywords: human aromatase, SNPs, phosphorylation, ST14A neuronal cells, MCF-7 breast cancer cells

1. Introduction

Human aromatase (CYP19A1) is a membrane-bound class II cytochrome P450 that converts androgens into estrogens [1-4]. Specifically, the enzyme is involved sex hormones biosynthesis where it is responsible for the conversion of androstenedione, testosterone and 16α-hydroxytestosterone into estrone, estradiol and estriol, respectively, through the aromatization of the A-ring of the steroid molecule with the subsequent release of the C19 as formic acid [1-3,5].

The enzyme is widely distributed within the human body, from ovaries to testis, brain, breast, adipose tissue, prostate, liver and bones. It is the product of one gene as a unique isoform and its wide distribution justifies its central role in different physiological processes [6]. Aromatase is not only responsible for sexual development and reproduction, but it plays also a key role in the maintenance of bone metabolism as well as in the neuroplasticity and neuroprotection of the brain [6-8]. In estrogen-deficient animal models, with a heterozygous disruption of ovarian aromatase gene, it was found that the decreased amount of estrogen levels was accompanied by an early formation and accumulation of β-amyloid plaques [9]. Moreover, aromatase protein is implicated in several pathologies, like breast cancer [6], polycystic ovary syndrome [10,11], endometrial cancer [12] and neurodegenerative pathologies such as Alzheimer's and Parkinson's diseases [13,14]. Such pathologies were proven to have a correlation with single nucleotide polymorphisms (SNPs) on the aromatase gene [10,15,16].

Out of the 7,000 SNPs described for *CYP19A1*, about 300 are located on the coding sequence and they are divided into frame shift, synonymous SNPs and missense substitutions. In 2001, through the expectation/maximization algorithm it was shown that aromatase gene is in linkage disequilibrium with Alzheimer's disease [17]. In 2006, different CYP19A1 haplotypes were correlated with an increased risk for Alzheimer's disease: the study of eighteen SNPs both in the 5' untranslated region and in the coding sequence of aromatase led to the hypothesis of an association between the onset of this neurodegenerative pathology and the APOE4 genotype carriers (apolipoprotein E, allele 4) [18]. SNPs occurring on the aromatase gene, however, were correlated also to other pathologies. One example is the case of the intron variant rs3764221 correlated to lung atypical adenomatous hyperplasia (AAH) and bronchioloalveolar carcinoma (BAC) and altered estrogens levels [19]. A case-control study showed that subjects carrying the intron variant rs1902584, located near the 1.4 promoter region, exhibit an increased risk to develop colorectal cancer [20]. Another case-control study conducted by using the luciferase reporter gene assay in PC3 and DU145 cancer cell lines showed that the intron variants rs2470152, rs10459592 and rs4775936 carrying the T-A-G haplotypes influence prostate cancer risk and survival by modifying

the activity of the 1.6 and PII promoters with subsequent effects on the sex hormones [21]. Moreover, it was also shown that Chinese Han women carrying the rs700518 AA genotype SNP involving Val80 are genetically susceptible to endometriosis-related infertility [22]. The same SNP was also associated with bone density loss in concomitance with aromatase inhibitors administration [23].

Out of the 300 SNPs located on the coding sequence of the CYP19A1 gene, the missense substitutions involving arginine 264 were selected in this work for functional studies. The choice was based on structural data showing that other aromatase polymorphisms, involving for instance W39, D309, R192 or the residues located in the D-E loop, can be predicted to generate an unfolded or inactive enzyme or a protein that does not correctly insert into the membrane [24,25]. Arginine 264, encoded by exon VII [26] and located on the G-helix [24,25], a region of cytochromes P450 characterised by high flexibility (Figure 1) [27] can be either found mutated into a histidine (SNP identification: rs2304462) or a cysteine (SNP identification: rs700519). Up to now, no studies are reported about the R264H polymorphism, while several and discordant are the literature data concerning the R264C SNP that is very common in Asian population [28,29].

In 1994, a case-control study reported that the R264C mutation did not affect breast cancer or fibroadenoma risk and *in vitro* experiments performed on breast cancer tissue showed that this mutation did not alter aromatase activity [30]. Similarly, it was shown that aromatase R264C SNP had no relationship with an increased breast cancer risk in Japanese women and did not affect the enzyme activity upon measurement of the radioactive activity of tritiated water released by transfected COS-7 cells [29]. In another study, the presence of this polymorphism was found to correlate with a higher risk for breast cancer that can be synergically increased by alcohol consumption [31]. In contrast, in 2005 it was assessed that the activity of aromatase transfected in COS-1 cells was reduced when cysteine is present in position 264 [26]. It was reported that the missense coding change R264C did not affect the concentration of serum estradiol in Australian women [32], while in Chinese women a case-control study evidenced that this aromatase SNP had no influence in endometrial cancer risk [12].

Here, the first aim of the this study is to compare the intrinsic properties (thermal stability and catalytic activity) of the two polymorphic variants to those of the wild type protein as well as a possible loss of consensus for phosphorylation by protein kinases A and G.

To this purpose, a recombinant and soluble form of human aromatase (rArom) [25,33-36], lacking the N-terminal helix, was used for site-directed mutagenesis to generate the two polymorphic variants rArom R264H and rArom R264C for functional studies on the purified enzymes.

The second aim of the study is to compare the activity of the variants to that of aromatase wild type

in two different cell lines. To this end, the full-length proteins were also expressed in two different eukaryotic cellular models, rat ST14A neuronal cells and human MCF-7 breast cancer cells, and the activity measured and compared.

2. Materials and Methods

2.1 Materials

All the chemicals were purchased from Sigma Aldrich and were analytical grade. Human cytochrome P450 reductase (hCPR) was purchased from Life Technologies.

2.2 Generation of the human aromatase polymorphic variants by site-directed mutagenesis

The experiments here proposed were performed on a recombinant soluble form of human aromatase (rArom) cloned in a pCW Ori+ vector carrying an IPTG-inducible Tac promoter, an ampicillin resistance gene and rArom cDNA cloned between NdeI and HindIII restriction sites at the five-prime and three-prime ends, respectively. Experiments were also performed on the full-length membrane-bound protein (Arom) cloned in a pCMV6-XL4 vector (Origene, Rockville, USA) carrying an ampicillin resistance gene and Arom cDNA cloned between NotI restriction sites both at the five-prime and three-prime ends. Empty pCMV6-XL4 vector (MOCK) was generated by self-circularisation after removing the gene cassette of full-length aromatase cDNA using a T4 DNA ligase (Thermo Scientific) following manufacturer recommendations.

The polymorphic variants of human aromatase R264H and R264C were generated using the QuikChange II site-directed mutagenesis kit (Agilent Technologies) using the following mutagenic primers: CTGATAGCAGAAAAAAGACACAGGATTTCCACAGAAGAG (forward) and CTCTTCTGTGGAAATCCTGTGTCTTTTTTCTGCTATCAG (reverse) for the aromatase R264H mutant and CTGATAGCAGAAAAAAGATGCAGGATTTCCACAGAAGAG (forward) and CTCTTCTGTGGAAATCCTGCATCTTTTTTCTGCTATCAG (reverse) for the aromatase R264C mutant.

Plasmid DNA was sequenced by Eurofins MWG Operon (Ebersberg, Germany).

2.3 Recombinant protein expression, purification and characterization by UV-vis spectroscopy.

The structurally and functionally well characterized recombinant form of human aromatase (rArom) was expressed and purified as previously described [33-36]. Briefly, transformed *E. coli* DH5 chemically-competent cells selected by 100 μg/mL ampicillin were induced by 0.5 mM IPTG and let grown 48 hours at 28°C in the presence of the heme precursor δ-aminolevulinic acid.

Cells were harvested and re-suspended in a 100 mM KPi pH 7.4, 20% glycerol, 0.1 % Tween-20 and 1 mM β-mercaptoethanol buffer supplemented with 1 mg/mL lysozyme, 1% Tween-20 and 1 mM PMSF (10 μM androstenedione was also added to co-purify the enzymes in the substrate-bound form) at 4°C, disrupted by sonication and ultra-centrifuged for 25 minutes at 40,000 rpm and 4°C in a Beckman Coulter Ultra centrifuge. rArom was purified by loading the supernatant on a diethylaminoethyl ion-exchange column (DEAE-Sepharose Fast-Flow, GE Healthcare) followed by a Nickel-ion affinity column (Chelating-Sepharose Fast-Flow, GE Healthcare). The protein was eluted applying a linear histidine gradient (1-40 mM) that was removed in Amicon Ultra 30,000 MWCO devices (Millipore).

CO-binding assay was performed in an Agilent 8453 UV-vis spectrophotometer (diode array). rArom at the final concentration of 1 μM was placed in a quartz cuvette in a 100 mM KPi pH 7.4, 20% glycerol, 0.1% Tween-20 and 1 mM β-mercaptoethanol buffer, saturated with 15 μM androstenedione, reduced by sodium dithionite until the α and β Soret bands joined and gently bubbled with carbon monoxide. The P450 content was calculated using a molar extinction coefficient (ε) at 450 nm of 91,000 M^{-1} cm^{-1} [37].

The binding constant (K_D) for the polymorphic variants and the substrate androstenedione were measured by Uv-vis spectroscopy. Substrate binding was monitored as a spectroscopic shift of the γ Soret peak from 418 nm to 394 nm in an Agilent 8453 UV-vis spectrophotometer (diode array) at the controlled temperature of 25°C (Agilent 89090 A Peltier). The rArom R264C and R264H variants (1.0 μM) were titrated with increasing concentrations of androstenedione (0.05 μM-15 μM) in a 100 mM KPi pH 7.4 buffer containing 20% glycerol, 0.1% Tween-20 and 1 mM β-mercaptoethanol. The dissociation constants K_D were calculated using the equation:

$\Delta A394\text{-}418 = \Delta A \text{ max } 394\text{-}418 \bullet [S]free / (K_D + [S]free)$

where [S]free is [S]total–[E·S] and [E·S] = ΔA394-418 [E]total / ΔAmax394-418.

2.4 Circular dichroism spectroscopy

The secondary structure of rArom WT and its two polymorphic variants was studied by circular dichroism spectroscopy in the far-UV range (200-240 nm), the region of the spectrum where the chromophores are the peptide bonds [38]. rArom was diluted to the final concentration of 2.5 μM in a 100 mM KPi pH 7.4, 20% glycerol, 0.1% Tween-20 and 1 mM β-mercaptoethanol buffer in a 0.1

cm pathlength cell and analysed at 25°C using a Jasco-815 instrument (Jasco Instrument). CD signals were converted into molar ellipticity according to the following equation: $[\theta] = [(\theta \times MRW)/(100 \times l \times C)]$, where θ is the observed signal in degrees at a concentration C (in g/ml) using a cell of pathlength l expressed in dm and MRW is the mean residue weight [39].

Circular dichroism spectroscopy was used to perform thermal denaturation experiments using 2.5 μM of rArom R264H and rArom R264C in their ligand-free and substrate-bound forms in a 100 mM KPi pH 7.4, 20 % glycerol, 0.1 % Tween-20 and 1 mM β-mercaptoethanol buffer in a Jasco-815 instrument (Jasco Instrument) using a 0.1 cm pathlength cell and raising the temperature from 30°C to 76°C allowing the sample to equilibrate for 3 minutes at each temperature before recording the spectrum in the far-UV range (200-240 nm).

The fraction of folded protein at 222 nm was plotted as a function of the temperature and data fitted to a single step transition curve from which the melting temperature (T_m) was derived according to the following equation: folded fraction = $a/(1+\exp(-T-T_m)/b)$, where a and b are fitting parameters. Each curve is the mean of three experiments.

2.5 Activity assay and kinetic parameters determination by HPLC

The kinetic parameters were determined by incubating rArom WT and the two polymorphic variants with different substrate concentrations followed by separation and quantification of the aromatase reaction product by HPLC analysis.

Reactions were set up by mixing 250 nM rArom, 250 nM hCPR, increasing androstenedione concentrations (0.5-20 μM) and 0.5 mM NADPH in a 100 mM KPi pH 7.0, 20% glycerol, 0.1% Tween-20 and 1 mM β-mercaptoethanol buffer. Reactions were carried out for ten minutes at 30°C, heat-inactivated for 10 minutes at 90°C and centrifuged for 5 minutes at 11,000*g* and room temperature.

The supernatant was collected and injected into a 1200 series HPLC apparatus (Agilent Technologies) using a ZORBAX Eclipse Plus C18 reverse phase column (Agilent Technologies).

Analytes were eluted applying an acetonitrile HPLC grade (Sigma Aldrich) linear gradient (5%-100%) mixed to filtered and degased MilliQ water at the flow rate of 0.5 mL/min.

A diode array detector set at the wavelengths of 237 nm and 280 nm was used to detect the substrate androstenedione and the product estrone, respectively.

Different estrone concentrations (0.2 μM-10 μM) were dissolved in a 100 mM KPi pH 7.0, 20% glycerol, 0.1% Tween-20 and 1 mM β-mercaptoethanol buffer to be injected into the HPLC system and build a calibration curve. The peaks were integrated and the corresponding areas plotted as a

function of the standard concentration resulting in a linear regression curve used for the quantification of the aromatase reaction product.

2.6 *In vitro* phosphorylation of recombinant human aromatase

In silico studies performed on the amino acidic sequence of rArom using the GPS 2.0 software [40] showed that six serine residues (S35, S36, S101, S102, S267 and S497) and four threonine residues (T35, T162, T268 and T392) are predicted to be sites of phosphorylation. In particular, the peptide comprised between R263 and K271 where R264 is located (-RRRISTEEK-) corresponds to the consensus motif for many different kinases, including the AGC-kinases PKA (consensus motif: -R-R-X-S/T-Φ-, where X is any amino acid and Φ is a hydrophobic residue) [41] and PKG1 (consensus motif: -X-R/K-R/K-X-S/T-X) [42]. In human aromatase sequence, Φ corresponds to a threonine (Thr268) and phosphorylation by PKA and PKG1 is predicted on both Ser267 and Thr268.

Purified rArom was phosphorylated using the active subunit of PKA (PKAcα, SignalChem) and the active subunit of PKG1 (PRPKG1, SignalChem) following strictly manufacturer instructions with one modification: labelled ATP was replaced by ATP (Sigma Aldrich). Kinases (23.2 nM PKA and 40 nM PKG1) diluted in the kinase dilution buffer (25 mM MOPS pH 7.2, 12.5 mM β-glycerol phosphate, 25 mM $MgCl_2$, 5 mM EGTA, 2 mM EDTA, 0.25 mM DTT, 5 % v/v glycerol. 50 ng/μL bovine serum albumin (BSA) were also added for PKA) were mixed with 3.6 μM rArom, cold distilled water and 50 μM ATP (10 μM cGMP was also added for PKG1). Reactions were carried out for 15 minutes at 30°C.

Negative control reactions were set up as described above by replacing PKA or PKG1 with the kinase dilution buffer. Positive control reactions were set up as it follows: PKA was selectively inhibited by adding to the reaction mixture 10 μM of the selective and potent inhibitor H89 (N-[2-(p-bromocinnamylamino)ethyl]-5-isoquinolinesulfonamide) [43] whereas PKG1 was selectively inactivated by omitting the activator cGMP from the reaction mixture.

For the activity assay, one aliquot of rArom was diluted in a tube containing 250 nM CPR and 10 μM androstenedione to a final concentration of 250 nM. The reaction was started by the addition of 0.5 mM NADPH and carried out for 10 minutes at 30°C. The reaction was heat-inactivated and injected into the HPLC for product quantification.

2.7 Western blot of phosphorylated rArom samples

Phosphorylated and non phosphorylated rArom samples (0.5 μg/sample) were denatured in boiling Laemmli buffer, resolved in a 10% SDS-PAGE and transferred onto a 0.45 μM nitrocellulose

membrane (GE Healthcare). A mouse primary monoclonal IgM anti-phosphoserine antibody (Catalogue number: sc-81514, batch number: L1511; Santa Cruz Biotechnology) and a mouse primary monoclonal IgG anti-phosphothreonine antibody (Catalogue number: sc-81526, batch number: J0510; Santa Cruz Biotechnology) were used diluted 1:200 in TBST 1X (150 mM NaCl, 10 mM Tris-HCl pH 7.4, 0.1% Tween-20) supplemented with 3 % w/v BSA. As secondary antibodies, a goat anti-mouse IgM HRP-linked (Catalogue number: sc-2064, batch number: J0113; Santa Cruz Biotechnology) and a goat anti-mouse IgG HRP-linked (Catalogue number: sc-2005, batch number: G1213; Santa Cruz Biotechnology) were used diluted 1:4,000 in TBST 1X supplemented with 1 % w/v BSA.

2.8 MCF-7 breast cancer cell culture, transient transfection and tritiated water release assay

Human MCF-7 breast cancer cells were used as the first eukaryotic cellular model to compare the activity of Arom WT and its two polymorphic variants. Cells were obtained from American Type Culture Collection and cultured in DMEM/F-12 medium supplemented with 5% newborn calf serum, 2 mmol/liter L-glutamine, and 50 U/ml penicillin/streptomycin. MCF-7 cells (ATCC) were limited to use within the first 10-15 passages from the original purchased vial. Cells were plated in 6-well plates and transiently transfected with 3 μg/well of empty or WT or R264C or R264H vectors using the FuGENE 6 Transfection Reagent (Promega), as recommended by the manufacturer. Aromatase activity was measured by tritiated water release assay, as previously described [44,45]. Total proteins were extracted using a lysis buffer containing 50 mM HEPES pH 7.5, 150 mM NaCl, 1.5 mM $MgCl_2$, 1 mM EGTA, 10% glycerol, 1% Triton X-100, and protease inhibitors (Sigma) and results obtained were expressed as picomoles per hour and normalized to mg of total proteins (pmol/h/mg total proteins).

2.9 ST14A neuronal cell culture: transient transfection and estrone competitive ELISA

The eukaryotic neuronal cell model used to compare the activity of the full-length aromatase polymorphic variants and the WT enzyme was the neural progenitor ST14A cell line, kindly provided by Professor Elena Cattaneo and derived from rat primary cells dissociated from embryonic day 14 striatal primordia as previously described [46]. 50,000 cells at passage number 8-10 were plated in 12-well format plates and grown as monolayers in Dulbecco's Modified Eagle Medium (DMEM) supplemented with 100 units/ml penicillin, 0.1 mg/ml streptomycin, 1 mM sodium pyruvate, 2 mM L-glutamine, and 10% heat-inactivated fetal bovine serum (FBS; Invitrogen), at the permissive temperature of 33°C in a 5% CO_2 atmosphere saturated with H_2O. After 24 hours, cells were transiently transfected in Opti-MEM reduced serum medium (Gibco) by

mixing 1.25 μg of DNA and 1.25 μL Lipofectamine2000 (Invitrogen) according to manufacturer recommendations.

Twenty-four hours post-transfection cells were stimulated in DMEM serum-free supplemented with 500 nM androstenedione for 2 hours at 33°C and 5% CO_2 atmosphere. After stimulation, 150 μL of the medium were collected and centrifuged at 1,000*g* and 4°C for 10 minutes to remove cellular debris without disrupting cells. 125 μL of the supernatant were collected and centrifuged for 10 minutes at 11,000*g* and room temperature to completely clarify the medium. The estrone containing supernatant was collected and analysed by direct competitive ELISA estrone Kit (Diagnostic Biochem Canada Inc.) following manufacturer instructions. Full-length aromatase activity was expressed as pmol estrone/hour/mg total proteins.

In parallel the 12-well format plates were washed with Dulbecco's Phosphate Buffered Saline (DPBS), carefully dried and stored at -80°C until protein extraction and western blot analysis.

2.10 Protein extraction and western blot analysis

Total cellular proteins of ST14A neuronal cells were extracted 24 hours post-transfection using RIPA buffer (0.5% sodium deoxycolate, 0.8% NaCl, 0.25% Tris-base, 0.06% EDTA, 0.1% SDS, 1% Triton X-100, 10% glycerol and 1X protease inhibitor cocktail (Roche) and quantified by Lowry assay [47]. Proteins (10 μg/sample) were denatured in boiling Laemmli buffer, resolved in a 10% SDS-PAGE and transferred onto a 0.45 μM polyvinylidene difluoride (PVDF) membrane (GE Healthcare). For immunoblotting a rabbit primary polyclonal anti-aromatase antibody kindly provided by Dr Harada (Fujita Health University, Nagoya, Japan) and a rabbit primary polyclonal anti-GAPDH antibody (Catalogue number: PA1-987; batch number: QE212271, Thermo Fisher) were used diluted 1:1,000 in TBST 1X supplemented with 5% BSA; as secondary antibody a goat anti-rabbit HRP-linked (Catalogue number: A16104; batch number: 46-183-082415; GE Healthcare) was used diluted 1:10,000 in TBST 1X supplemented with 5% nonfat dry milk.

Total cellular proteins (40 μg/sample) extracted from MCF-7 breast cancer cells were denatured in boiling Laemmli buffer, resolved in a 10% SDS-PAGE and transferred onto a 0.2 μM nitrocellulose membrane (GE Healthcare). For immunoblotting a mouse monoclonal primary antibody anti-aromatase (Catalogue number MCA20775, Clone H4; batch number: 240914; Serotec) and a rabbit monoclonal primary antibody anti-GAPDH (catalogue number: sc-25788, FL-335, batch number: 10413, Santa Cruz Biotechnology) were used at 1:500 and 1:10,000 dilution, respectively, in TBST 1X supplemented with 5% BSA; as secondary antibodies, a goat anti-mouse and anti-rabbit HRP-linked (Santa Cruz Biotechnology) were used at 1:2,000 and 1:7,000 dilution, respectively, in TBST

1X supplemented with 5% BSA. Immunoblots show a single representative of 3 indipendent experiments.

3. Results

3.1 UV-vis spectroscopy, folding and thermal stability of rArom R264C and R264H variants.

The expression and purification of the rArom WT and the two polymorphic variants rArom R264C and rArom R264H were achieved as reported for recombinant human aromatase (rArom) [33,34]. The UV-vis spectra of the three proteins used in this study in their substrate-free and substrate-bound forms are shown in Figure 2. The purified ligand-free proteins show the typical low-spin spectrum with the maximum Soret peak at 418 nm and α and β bands centred at 570 nm and 535 nm, respectively (Figures 2A, 2B and 2C). In the case of the enzymes co-purified with the substrate androstenedione, the typical high spin spectrum was observed, exhibiting the maximum absorbance peak at 394 nm and the α and β bands to 512 and 542 nm respectively, with a charge transfer band at 645 nm typical of the iron in a high spin state (Figure 2A, 2B and 2C). Thus, the substrate androstenedione induces the typical low-to-high spin transition of the heme iron. Moreover, the CO-binding assay was performed and upon reduction with sodium dithionite and bubbling with carbon monoxide, the difference spectra Fe(II)-CO minus Fe(II) of the aromatase samples showed the typical peak at 450 nm (insets in Figure 2A, 2B and 2C).

Enzyme folding was then studied by circular dichroism spectroscopy. The secondary structure of the three proteins both in the ligand-free and substrate-bound forms was compared and no major differences were observed for both the polymorphic variants compared to rArom WT (Figure 2D), indicating that the R-to-H/C substitutions do not alter the secondary structure composition of the polymorphic enzymes also in the presence of the substrate androstenedione. Moreover, a molar ellipticity of -18,000 degrees cm^2 $dmol^{-1}$ at 222 nm is representative for an α-helices content of 52% [39], consistent with the value calculated from the crystal structure of rArom WT [25].

The thermal stability of the three enzymes was studied by thermal denaturation experiments monitoring the loss of secondary structure by circular dichroism spectroscopy. The unfolding process followed a typical cooperative single step sigmoidal curve in all cases (Figure S1). As previously observed in other cytochromes P450 [48], the process was also found to be irreversible suggesting protein aggregation during denaturation and loss of the heme cofactor. T_m values (Table 1) are found to be within the range of those reported for other mammalian cytochromes P450 [49]. Ligand-free rArom R264C and R264H showed a melting temperature lowered by 3 and 5 °C compared to rArom WT, respectively. The presence of androstenedione was found to stabilise the

protein structure in all cases by increasing their thermal stability by 3-4 °C.

These results are in line with crystallographic data reporting that the presence of the substrate stabilises the structure of cytochromes P450 by reducing the flexibility of key region involved in substrate binding and recognition such as the F-G loop [50,51].

3.2 Binding constants and kinetic parameters determination

Difference spectroscopy was used to determine the binding constant (K_D) of the two polymorphic variants rArom R264H and rArom R264C for the substrate androstenedione. For both variants, the resulting K_D values resulted 2-folds higher than the one calculated for rArom WT (Table 1) indicating a loss in the binding ability for the substrate when the mutation is present.

The kinetic parameters for the three proteins were also calculated. The plots of estrone formation rate as a function of substrate concentration are reported in Figure S2, where a hyperbolic trend consistent with a Michaelis-Menten behaviour was observed for all the three recombinant enzymes. The calculated kinetic parameters are reported in Table 1. When compared to rArom WT, the polymorphic variant rArom R264H exhibited a 2.5 folds higher K_M and a 1.4 folds lower k_{cat} value. On the contrary, rArom R264C shows a 1.6 fold higher K_M constant and a k_{cat} similar to rArom. As a consequence, rArom R264H shows a 3.4 folds lower catalytic efficiency whereas rArom R264C exhibits a k_{cat}/K_M ratio decreased by a factor of 1.5. Thus, despite the polymorphism involving R264 is localised on the surface of the protein, the Arg-to-His/Cys substitutions are found to have an influence on key functional parameters of human aromatase.

3.3 Effect of *in vitro* phosphorylation on rArom activity

Since PKA and PKG1 are predicted to phosphorylate aromatase on Ser267 and Thr268, the purified recombinant proteins were phosphorylated by these two selected kinases and the activity was measured before and after phosphorylation.

The results of western blot analysis using anti-phosphoserine and anti-phosphothreonine antibodies (Figure 3A) shows that the three proteins are phosphorylated in serine and threonine upon treatment with both PKA and PKG, confirming the *in silico* predictions.

The results of the activity assays of the phosphorylated and non-phosphorylated proteins are shown in Figure 3B. Upon phosphorylation with PKA, the activity of rArom decreased in all cases, but to a different extent: rArom R264C lost 49.3% of its original activity, while the activity of rArom and rArom R264H was found to be affected by 36.2% and 27.9%, respectively (Figure 3B; Table 2). When the same experiment was performed in the presence of H89, a synthetic and specific inhibitor

of PKA, the activity of rArom resulted to be restored confirming that the decrease previously observed was due to PKA-dependent phosphorylation (Figure 3B; Table 2).

Similar results were obtained upon phosphorylation of rArom using the catalytic subunit of PKG1 where the activity of aromatase decreased in all cases, but to a generally minor extent when compared to PKA. The variant rArom R264H lost 15.4% of its original activity upon phosphorylation, while rArom WT and rArom R264C lost 30.5% and 30.3% of their original activity, respectively (Figure 3A; Table 2). When the same experiment was performed in the absence of cGMP, required for PKG1 activation [52], no variations in rArom activity were observed, implicating that also PKG1 modulates enzyme activity through a phosphorylation-dependent inhibition (Figure 3A; Table 2).

These data indicate that human aromatase and the polymorphic variants are inhibited by phosphorylation by PKA and PKG and that the substitution of R264C/H affects the phosphorylation rate depending on the kinase considered.

3.4 Full-length aromatase (Arom) activity in ST14A neuronal cells and MCF-7 breast cancer cells

The effects of phosphorylation found in the activity of the recombinant purified enzymes where then investigated in the full-length human enzyme, wild type and polymorphic variants, in two different eukaryotic cellular models.

Human MCF-7 breast cancer cells were chosen due to the central role of aromatase in catalysing local estrogen production, that is an important mechanism of autocrine and paracrine growth stimulation in hormone-dependent breast cancers. The neuronal progenitor of rat striatum ST14A cells, indeed, was chosen since the enzyme is known to be expressed in several regions of the cerebral cortex where estrogens act as neuroprotective in case of stroke and brain injury and participate in neuroplasticity [8].

For in cell activity assays, human WT or variant full length aromatase cDNAs were transiently transfected in both eukaryotic cellular models, where the presence of the enzymes was verified by immunoblotting using GAPDH as housekeeping protein (Figures 4B and 4D). After 2 hours of stimulation with labelled androstenedione as substrate, aromatase activity was measured by tritiated water release method. The specific activity of both polymorphic variants in human MCF-7 breast cancer cells was found to be significantly different with respect to the WT (Figure 4A). Arom R264H exhibited a 1.6 fold higher activity, while Arom R264C showed a 1.6 fold lower activity. In contrast, upon two hours treatment with androstenedione, the specific activity of the three enzymes did not show any significant difference in ST14A neuronal cells (Figure 4C). It is important to

underline that, although the house keeping protein GAPDH showed the same expression levels in all transfected samples, Arom R264H showed expression levels comparable to Arom WT, while Arom R264C resulted to be less expressed in both cell lines (Figure 4B and D). Such differences could suggest a lower stability or a faster degradation rate for the aromatase R264C variant in our cellular models.

4. Discussion

The study of the effect of polymorphisms on key enzymes of the endocrine and neuroendocrine systems such as on the aromatase, can be crucial to understand the relationship between SNPs and increased/decreased risk for pathologies. Although the effect of some SNPs on the coding sequence can be predicted by analysis of the crystal structure combined with functional studies, the alterations produced by non-active site and surface mutations such as R264C/H in human aromatase is not obvious. For this reason, the availability of recombinant and purified proteins is a powerful tool to compare kinetic parameters and to perform assays where proteins potentially altering aromatase activity can be selectively used.

In this work, polymorphisms involving arginine 264, located on the G-helix [24,25], a region of cytochromes P450 characterised by high flexibility [27], were studied.

Despite both the mutations occurring on R264 are classified as aromatase single nucleotide polymorphisms [18], no literature data are so far available regarding the R264H substitution. On the contrary, several and discordant are the literature reports about the R264C polymorphism [12,26,28,30,32].

The two polymorphic variants displayed similar secondary structure content but a lower thermal stability compared to rArom WT. A lower thermal stability is usually associated to a higher flexibility that may result in a loss of affinity for substrates and reduced catalytic rate. As a matter of the fact, the K_D values for the polymorphic variants are 2-folds higher compared to rArom WT and the catalytic efficiency resulted lowered by 1.5 and 3.4 for R264C and R264H, respectively.

Molecular dynamics simulations on human aromatase have previously shown that helix G, where Arg264 is located, is flexible and it is part of the substrate access channel [53-55]. Moreover, in other cytochromes P450, x-ray crystallography has shown that surface mutations can influence not only the flexibility of structural elements important for substrate access but they can also exert structural long-range effect influencing active site residues important for substrate recognition [56].

Moreover, since R264 is part of a consensus sequence for phosphorylation by different kinases, it is predictable that the mutations affect such a consensus. Phosphorylation experiments showed that upon treatment with PKA and PKG1, the activity of rArom R264H is the least affected in terms of

estrone production (Figure 6; Table 3), suggesting a partial loss of consensus for PK recognition. The different loss of activity upon phosphorylation by PKA and PKG can be explained by the different consensus score obtained from *in silico* predictions on both Ser267 and Thr268. Thus, the binding constant as well as phosphorylation rates can be different according to the kinase/residue involved.

rArom WT and rArom R264C, indeed, were found both to be more affected upon this post-translational modification. These data are in line with previous findings reported for homogenates of quail brain full-length aromatase, where a rapid down-regulation of aromatase activity (47% of activity lost) was observed within minutes upon stimulation with the specific kinase activators ATP, Mg^{2+} and Ca^{2+}, necessary to activate PKA. Moreover, the same experiments performed in the presence of H89 resulted in the total recovery of aromatase activity [57-59] as in the case of the experiments performed on rArom and the two variants.

Human aromatase phosphorylation by PKA is known to occur on different serine and threonine residues and the enzyme activity is the result of the overall phosphorylation status of the protein on multiple sites [60]. Post-translational regulation of aromatase by phosphorylation processes was also reported in breast cancer [61]. For instance, 17-β estradiol exposure promotes aromatase phosphorylation at Tyr361 in breast cancer cells, enhancing enzyme activity with subsequent carcinogenic cell proliferation [62]. Recently it was also reported that aromatase in JEG3 cells is rapidly inactivated and subsequently degraded upon calcineurin-dependent phosphorylation promoted by calcium calmodulin kinase II [63].

The activity of the three proteins was also studied in their full-length upon transient transfection in two eukaryotic cellular models: human MCF-7 breast cancer cells and rat ST14A neuronal cells. In the MCF-7 cells, Arom R264H showed the same expression levels as Arom WT but it exhibited also significantly higher activity, in line with the results obtained using the purified proteins, where this variant is the least inhibited upon phosphorylation. The variant Arom R264C was found to be significantly less active with a concomitant lower expression level (Figures 6A and 6B). Since the mutation is in the coding sequence and the promoter region is unaltered, this result suggests that this variant is less stable in the cell and faster degraded. Since it is known that phosphorylation triggers ubiquitination in human cytochromes P450 [64] and the variant R264C is the most affected in terms of activity by phosphorylation by PKA, it may be hypothesised that the cysteine mutation increases the consensus for selected kinases that decrease the half life of this protein in cells. A similar result was also observed in ST14A cells, where the Arom R264C amount is lower compared to wild type and R264H (Figure 4D). Interestingly, in these cells no significant differences were found when comparing the activity of the three full-length aromatase proteins (Figure 4C). Thus, depending on

the eukaryotic cellular model under investigation, human aromatase polymorphic variants exhibits different behaviours compared to WT, probably related to post-translational modifications and/or different protein stability.

However, it has to be taken into account that Arg264 is part of the consensus sequence for many different Ser/Thr kinases. As a future perspective, all these proteins can be screened on the purified enzyme to understand which ones act on aromatase. These data can be then complemented with experiments where cells are treated with selective kinases activators/inhibitors in order to draw a more complete picture about post-translational modifications affecting aromatase activity in specific cell lines.

In conclusion, the results here presented show that biochemical methodologies and cell biology techniques allow to combine intrinsic structural and functional properties of human aromatase with cellular regulatory mechanisms. All these factors can have different synergic or antagonist effects on the enzyme and its polymorphic variants that may affect local estrogens concentrations that are crucial for the development of many diseases.

Acknowledgements

This work was supported by the FIRB grant 2012 Programme "Futuro in Ricerca" project RBFR12FI27_004 to Giovanna Di Nardo and RBFR12FI27_001 to Ines Barone).

References

1. E.A.J. Thompson, P.K. Siiteri, The involvement of human placental microsomal cytochrome P-450 in aromatization, J. Biol. Chem. 249 (1974a) 5373-5378.

2. E.A.J. Thompson, P.K. Siiteri, Utilisation of oxygen and reduced nicotinamide adenine dinucleotide phosphate by human placental microsomes during aromatization of androstenedione, J. Biol. Chem. 249 (1974b) 5364-5372.

3. E. Simpson, M. Mahendroo, G. Means, M. Kilgore, M. Hinshelwood, S. Graham-Lorence, B. Amarneh, Y. Ito, C. Fisher, M. Michael, Aromatase cytochrome P450, the enzyme responsible for estrogen biosynthesis, Endocr. Rev. 15 (1994) 342–55.

4. F. Hannemann, A. Bichet, K.M. Ewen, R. Bernhardt, Cytochrome P450 systems-biological variations of electron transport chain, Biochim. Biophys. Acta 1770 (2007) 330-344.

5. G. Di Nardo, G. Gilardi, Human aromatase: perspectives in biochemistry and biotechnology, Biotechnol. Appl. Bioch. 60 (2013) 92-101.

6. R.J. Santen, H. Brodie, E.R. Simpson, P.K. Siiteri, A. Brodie, History of aromatase: saga of an important biological mediator and therapeutic target, Endocr. Rev. 30 (2009) 343-375.

7. C.F. Roselli, Brain aromatase: roles in reproduction and neuroprotection, J. Steroid. Biochem. 106 (2007) 143-150.

8. E.D. Lephart, T.D. Lund, T.L. Horvath, Brain androgen and progesterone metabolizing enzymes: biosynthesis, distribution and function, Brain. Res. Rev. 37 (2001) 25-37.

9. X. Yue, M. Lu, T. Lancaster, P. Cao, S.I. Honda, M. Staufenbiel, N. Harada, Z. Zhong, Y. Shen, R. Li,. Brain estrogen deficiency accelerates Aβ plaque formation in an Alzheimer's disease animal model, Proc. Natl. Acad. Sci. U.S.A. 102 (2005) 19198-19203.

10. N. Xita, L. Lazaros, I. Georgiou, A. Tsatsoulis, CYP19 gene: a genetic modifier of polycystic ovary syndrome phenotype, Fertil. Steril. 94 (2010) 250-254.

11. P. Xu, X.L. Zhang, G.B. Xie, C.W. Zhang, S.M. Shen, X.X. Zhang, Y.X. Cao, W.J. Wang, Y.N. Che, Y.J. Xia, X.K. Wu, L. Yi, Q. Gao, Y. Wang, The $(TTTA)_n$ polymorphism in intron 4 of *CYP19* and the polycystic ovary syndrome risk in a Chinese population, Mol. Biol. Rep. 40 (2013) 5041-5047.

12. M.H. Tao, Q. Cai, Z. Zhang, W. Xu, N. Kataoka, W. Wen, Y. Xiang, W. Zhenh, X.O. Shu, Polymorphisms in the *CYP19A1* (aromatase) gene and endometrial cancer risk in Chinese women, Cancer Epidem. Biomar. 16 (2007) 943-949.

13. J.W. Simpkins, P.S. Green, K.E. Gridley, M. Singh, N.C. de Fiebre, G. Rajakumar, Role of estrogen replacement therapy in memory enhancement and the prevention of neuronal loss associated with Alzheimer's disease, Am. J. Med. 103 (1997) 19S-25S.

14. C. Leranth, R.H. Roth, J.D. Elsworth, F. Naftolin, T.L. Horvath, D.E. Redmond, Estrogen is essential for maintaining nigrostriatal dopamine neurons in primates: implications for Parkinson's disease and memory, J. Neurosci. 20 (2000) 8604-8609.

15. M. Hiltunen, S. Iivonen, H. Soininen, Aromatase enzyme and Alzheimer's disease, Minerva Endocrinol. 31 (2006) 61-73.

16. C. Medway, O. Combarros, M. Cortina-Borja, H.T. Butler, C.A. Ibrahim-Verbaas, R.F.A.G. de Bruijn, P.J. Koudstaal, C.M. van Duijn, M.A. Ikram, I. Mateo, P. Sánchez-Juan, M.G. Lehmann, R. Heun, H. Kölsch, P. Deloukas, N. Hammond, E. Coto, V. Alvarez, P.G. Kehoe, R. Barber, G.K. Wilcock, K. Brown, O. Belbin, D.R. Warden, A.D. Smith, K. Morgan, D.J. Lehmann, The sex-specific associations of the aromatase gene with Alzheimer's disease and its interaction with *IL10* in the epistasis project, Eur. J. Hum. Genet. 22 (2014) 216-220.

17. S. Iivonen, E. Corder, M. Lehtovirta, S. Helisalmi, A. Mannermaa, S. Vepsäläinen, T. Hänninen, H. Soininen, M. Hiltunen, Polymorphisms in the CYP19 gene confer increased risk for Alzheimer's disease, Neurology 62 (2004) 1170-1176.

18. R. Huang, S.E. Poduslo, CYP19 haplotypes increase risk for Alzheimer's disease, J. Med. Genet. 43 (2006) e42.

19. T. Kohno, R. Kakinuma, M. Iwasaki, T. Yamaji, H. Kunitoh, K. Suzuki, Y. Shimada, K. Shiraishi, Y. Kasuga, G.S. Hamada, K. Foruta, K. Tsuta, H. Sakamoto, A. Kuchiba, S. Yamamoto, Y. Kanai, S. Tsugane, J. Yokota, Association of *CYP19A1* polymorphisms with risks for atypical adenomatous hyperplasia and bronchioloalveolar carcinoma in the lungs, Carcinogenesis 31 (2010) 1794-1799.

20. J.H. Lin, J.E. Manson, P. Kraft, B.B. Cochrane, M.J. Gunter, R.T. Chlebowski, S.M. Zhang, Estrogen and progesterone-related gene variants and colorectal cancer risk in women, B.M.C. Med. Genet. 12 (2011) 78-86.

21. S. Kanda, N. Tsuchiya, S. Narita, T. Inoue, M. Huang, S. Chiba, S. Akihama, M. Saito, K. Numakura, H. Tsuruta, S. Satoh, S. Saito, C. Ohyama, Y. Arai, O. Ogawa, T. Habuchi, Effects of functional genetic polymorphisms in the *CYP19A1* gene on prostate cancer risk and survival, Int. J. Cancer 136 (2014) 74-82.

22. L. Wang, X. Lu, D. Wang, W. Qu, W. Li, X. Xu, Q. Huang, X. Han, J. Lv, *CYP19* gene variant confers susceptibility to endometriosis-associated infertility in Chinese women, Exp. Mol. Med. 46 (2014) e103.

23. N. Napoli, A. Rastelli, C. Ma, J. Yarramaneni, S. Vattikutti, G. Moskowitz, T. Giri, C. Mueller, V. Kulkarny, C. Qualls, M. Ellis, R. Armamento-Villareal, Genetic polymorphism at Val^{80} (rs700518) of the CYP19A1 gene is associated with aromatase inhibitor associated bone loss in women with ER (+) breast cancer, Bone 55 (2013) 309-314.

24. D. Ghosh, J. Griswold, M. Erman, W. Pangborn, Structural basis for androgen specificity and oestrogen synthesis in human aromatase, Nature 457 (2009) 219-23.

25. J. Lo, G. Di Nardo, J. Griswold, C. Egbuta, W. Jiang, G. Gilardi, D. Ghosh, Structural basis for the functional roles of critical residues in human cytochrome P450 aromatase, Biochemistry 52 (2013) 5821-5829.

26. C.X. Ma, A.A. Adjei, O.E. Salavaggione, J. Coronel, L. Pelleymounter, L. Wang, B.W. Eckloff, D. Schaid, E.D. Weiben, R.M. Weinshilboum, Human aromatase: gene sequencing and functional genomics, Cancer Res. 65 (2005) 11071-11082.

27. P.R. Ortiz de Montellano, Cytochrome P450. Structure, mechanism, and biochemistry, fourth ed., Springer, New York, 2015.

28. J. Watanabe, N. Harada, K. Suemasu, Y. Higashi, O. Gotoh, K. Kawajiri, Arginine-cysteine polymorphism at codon 264 of the human CYP19 gene does not affect aromatase activity, Pharmacogenomics 7 (1997) 419-424.

29. Y. Miyoshi, K. Iwao, N. Ikeda, C. Egawa, S. Noguchi, Breast cancer risk associated with polymorphism in *CYP19* in Japanese women, Int. J. Cancer (Pred. Oncol.) 89 (2000) 325-328.

30. P. Sourdaine, M.G. Parker, J. Telford, W.R. Miller, Analysis of the aromatase cytochrome P450 gene in human breast cancers, J. Mol. Endocrinol. 13 (1994) 331-337.

31. K.M. Lee, J. Abel, Y. Ko, V. Harth, W.Y. Park, J.S. Seo, K.Y. Yoo, J.Y. Choi, A. Shin, S.H. Ahn, D.Y. Noh, A. Hirvonen, D. Kang, Genetic polymorphisms of cytochrome P450 19 and 1B1, alcohol use, and breast cancer risk in Korean women, Brit. J. Cancer 88 (2003) 675-678.

32. J.Z. Wang, M.S. Deogan, J.R. Lewis, S. Chew, B.H. Mullin, T.J. McNab, S.G. Wilson, E. Ingley, R.L. Prince, A non-synonymous coding change in the CYP19A1 gene R264C (rs700519) does not affect circulating estradiol, bone structure or fracture, B.M.C. Med. Genet. 12 (2011) 165.

33. G. Di Nardo, M. Breitner, S. Sadeghi, S. Castrignanò, G. Mei, A. Di Venere, E. Nicolai, P. Allegra, G. Gilardi, Dynamics and flexibility of human aromatase probed by FTIR and time resolved fluorescence spectroscopy, PLoS ONE 8 (2013) e82118.

34. G. Di Nardo, M. Breitner, A. Bandino, D. Ghosh, G.K. Jennings, J.C. Hackett, G. Gilardi, Evidence for an elevated aspartate pK_a in the active site of human aromatase, J. Biol. Chem. 290 (2015) 1186-1196.

35. G. Di Nardo, S. Castrignanò, S.J. Sadeghi, R. Baravalle, G. Gilardi, Bioelectrochemistry as a tool for the study of aromatization of steroids by human aromatase, Electrochem. Commun. 52 (2015) 25-28.

36. S. Maurelli, M. Chiesa, E. Giamello, G. Di Nardo, V.E.V. Ferrero, G. Gilardi, S. Van Doorslaer, Direct spectroscopic evidence for binding of anastrozole to the iron heme of human aromatase. Peering into the mechanism of aromatase inhibition, Chem. Commun. 47 (2011) 10737-10739.

37. T. Omura, R. Sato, The carbon-monoxide binding pigment of liver microsomes: I. Evidence for its hemoprotein nature, J. Biol. Chem. 239 (1964) 2370-2378.

38. S.M. Kelly, T.J. Jess, N.C. Price, How to study proteins by circular dichroism, Biochim. Biophys. Acta 1751 (2005) 119-139.

39. Y. Chen, J.T. Yang, K.H. Chau, Determination of the helix and β form of proteins in aqueous solution by circular dichroism, Biochemistry 13 (1974) 3350-3359.

40. Y. Xue, J. Ren, X. Gao, C. Jin, L. Wen, X. Yao, GPS 2.0, a tool to predict kinase specific phosphorylation in hierarchy, Mol. Cell. Proteomics 7 (2008) 1598-1608.

41. J.A. Ubersax, J.E.J Ferrell, Mechanism specificity in protein phosphorylation, Nature 8 (2007) 530-541.

42. M.G. Johlfs, R.R. Fiscus, Protein kinase G type I-α phosphorylates the apoptosis regulating protein Bad at serine 155 and protects against apoptosis in N1E-115 cells, Neurochem. Int. 56 (2010) 546-553.

43. T. Chijiwa, A. Mishima, M. Hagiwara, M. Sano, K. Hayaishi, T. Inoue, K. Naito, T. Toshioka, H. Hidaka, Inhibition of forskolin-induced neurite outgrowth and protein phosphorylation by a newly synthesised selective inhibitor of cyclic AMP-dependent protein kinase, N-[2-(p-bromocynnamilamino)ethyl]-5-isoquinolinesulfonamide (H89), of PC12D pheochromocytoma cells, J. Biol. Chem. 265 (1990) 5267-5272.

44. E.D. Lephart, E.R. Simpson, Assay of aromatase activity, Methods Enzymol. 206 (1991) 477-483.

45. I. Barone, C. Giordano, R. Malivindi, M. Lanzino, P. Rizza, I. Casaburi, D. Bonofiglio, S. Catalano, S. Andò, Estrogens and PTP1B function in a novel pathway to regulate aromatase enzymatic activity in breast cancer cells, Endocrinology 153 (2012) 5157-66.

46. E. Cattaneo, L. Conti, Generation and characterization of embryonic striatal conditionally immortalised ST14A cells, J. Neurosci. Res. 53 (1998) 223-234.

47. O.H. Lowry, N.J. Rosebrough, A.L. Farr, R.J. Randall, Protein measurement with the Folin phenol reagent, J. Biol. Chem. 193 (1951) 265-275.

48. S. Kumar, Y. Zhao, L. Sun, S.S. Negi, J.L. Halpert, B.K. Muralidhara, Rational engineering of cytochrome P450 2B6 for enhanced expression and stability: importance of a Leu264->Phe substitution, Mol. Pharmacol. 72 (2007) 1191-1199.

49. S. Kumar, L. Sun, H. Liu, B.K. Muralidhara, J.R. Halpert, Engineering mammalian cytochrome P4502B1 by directed evolution for enhanced catalytic tolerance to temperature and dimethyl sulfoxide, Prot. Eng. Des. Sel. 19 (2006) 547-554.

50. H. Li, T.L. Poulos, Modelling protein-structure interactions in the heme domain of cytochrome P450 (BM-3), Acta Crystallogr. D 51 (2005) 21-32.

51. T.W. Ost, J. Clark, C.G. Mowat, C.S. Miles, M.D. Walkinshaw, G.A. Reid, S.K. Chapman, S. Daff, Oxygen activation and electron transfer in flavocytochrome P450 BM3, J. Am. Chem. Soc. 125 (2003) 15010-15020.

52. S.H. Francis, J.L. Busch, J.D. Corbin, cGMP-dependent protein kinases and cGMP phosphodiesterases in nitric oxide and cGMP action, Pharmacol. Rev. 62 (2010) 525-563.

53. J. Sgrignani, A. Magistrato, Influence of the membrane lipophilic environment on the structure and on the substrate access/egress routes of the human aromatase enzyme. A computational study, J. Chem. Inf. Model. 2 (2012) 1595–1606.

54. J. Park, L. Czapla, R.E. Amaro, Molecular simulations of aromatase reveal new insights into the mechanism of ligand binding, J. Chem. Inf. Model. 53 (2013) 2047-56.

55. W. Jiang, D. Ghosh D, Motion and flexibility in human cytochrome p450 aromatase, PLoS One 7 (2012) e32565.

56. G. Di Nardo, V. Dell'Angelo, G. Catucci, S.J. Sadeghi, G. Gilardi, Subtle structural changes in the Asp251Gly/Gln307His P450 BM3 mutant responsible for new activity toward diclofenac, tolbutamide and ibuprofen, Arch. Biochem. Biophys. 602 (2016) 106-115.

57. J. Balthazart, M. Baillien, F.G. Ball, Phosphorylation processes mediate rapid changes of brain aromatase activity, J. Steroid. Biochem. 79 (2001) 261-277.

58. J. Balthazart, M. Baillien, T.D. Charlier, F.G. Ball, Calcium-dependent phosphorylation processes control brain aromatase in quail, Eur. J. Neurosci. 17 (2003) 1591-1606.

59. J. Balthazart, M. Baillien, F.G. Ball, Interactions between kinases and phosphatases in the rapid control of brain aromatase, J. Endocrinol. 17 (2005) 553-559.

60. T.D. Charlier, N. Harada, J. Balthazart, C.A. Cornil, Human and quail aromatase activity is rapidly and reversibly inhibited by phosphorylating conditions, 152 (2011) 4199–4210.

61. S. Catalano, I. Barone, S. Marsico, R. Bruno, S. Andò , Phosphorylation processes controlling aromatase activity in breast cancer: an update, Mini Rev Med Chem. 16 (2016) 691-698.

62. S. Catalano, I. Barone, C. Giordano, P. Rizza, H. Qi, G. Gu, R. Malivindi, D. Bonofiglio, S. Andò, Rapid estradiol/ERα signalling enhances aromatase enzymatic activity in breast cancer cells, Mol. Endocrinol. 23 (2009) 1634-1645.

63. T. Hayaishi, N. Harada, Post-translational dual regulation of cytochrome P450 aromatase at the catalytic and protein levels by phosphorylation/dephosphorylation, FEBS J. 281 (2014) 4830-4840.

64. Y. Wang, M. Liao, N. Hoe, P. Acharya, C. Deng, A.N. Krutchinsky, M.A. Correia, A role for protein phosphorylation in cytochrome P450 3A4 ubiquitin-dependent proteasomal degradation, J. Biol. Chem. 284 (2009) 5671-5684.

Figures legends

Figure 1. Arg264 is located in helix G, an element with high B-factor. Crystal structure of recombinant human aromatase (rArom; PDB ID: 4KQ8) coloured according to the B-factor: a low B-factor (< 54 $Å^2$) is shown in blue; a high B-factor (> 131 $Å^2$) is shown in red. Side chain of arginine 264 is also shown in the green circle.

Figure 2. The purified polymorphic variants show spectroscopic properties similar to purified rArom WT. Visible spectra showing 0.8 μM ligand-free (black trace) and 0.8 μM androstenedione-bound (grey trace) rArom WT (A), 0.8 μM ligand-free (black trace) and 0.8 μM androstenedione-bound (grey trace) rArom R264H (B) and 0.8 μM ligand-free (black trace) and 0.8 μM androstenedione-bound (grey trace) rArom R264C (C). Insets: Fe(II)-CO minus Fe(II) difference spectrum obtained upon CO-binding assay performed on 1 μM freshly purified rArom. D) Far-UV circular dichroism spectra acquired on 2.5 μM ligand-free rArom WT (solid line), 2.5 μM ligand-free rArom R264H (long dashed line) and 2.5 μM ligand-free rArom R264C (dotted line).

Figure 3. PKA and PKG phosphorylate aromatase and the polymorphic variants at a different level. A) Western blot analysis performed on 0.5 μg rArom WT (lanes 1), 0.5 μg rArom R264H (lanes 2) and 0.5 μg rArom R264C (lanes 3) after *in vitro* phosphorylation. Lanes 4: negative control. Left top panel shows immunoblot performed on rArom treated with PKA using a mouse primary antibody to α-phosphoserine residues. Right top panel shows immunoblot performed on rArom treated with PKA using a mouse primary antibody to α-phosphothreonine residues. Left bottom panel shows immunoblot performed on rArom treated with PKG1 using a mouse primary antibody to α-phosphoserine residues. Right bottom top panel shows immunoblot performed on rArom treated with PKG1 using a mouse primary antibody to α-phosphothreonine residues.
B) Effect on the activity of rArom WT (white bars), rArom R264H (light grey bars) and rArom R264C (dark grey bars) in the presence of 40 ng of PKA, in the presence of 40 ng PKA and 10 μM H89, in the presence of 100 ng PKG1 and in the presence of 100 ng PKG1 and in the absence of cGMP. Basal activity of the three enzymes is also shown (control). Data points are the average of four independent experiments and error bars represent the standard deviation. * P-value < 0.05 by one-way ANOVA and ** P-value < 0.001 by one-way ANOVA refer to samples treated with kinases rArom compared to controls. $^{\#}$ P-value < 0.05 by one-way ANOVA and $^{\#\#}$ P-value < 0.001 by one-way ANOVA refer to the polymorphic variants treated with kinases compared to rArom WT treated with kinases.

Figure 4. The polymorphic variants R264C and R264H have a different expression and activity compared to aromatase wild type according to the cell line used. A) Specific activity of aromatase in human MCF-7 breast cancer cells transiently transfected with empty vector (MOCK), full-length aromatase WT, full-length aromatase R264H or full-length aromatase R264C. Data points are the average of three independent measurements and error bars represent the standard deviation. * P-value < 0.05 by one-way ANOVA. ** P-value < 0.005 by one-way ANOVA. B) Western blot analysis performed on 40 µg total cellular proteins extracted from human MCF-7 breast cancer cells transiently transfected with empty vector (MOCK, lane 1), or human MCF-7 cells transiently transfected with full-length aromatase WT (lane 2), full-length aromatase R624H (lane 3) and full-length aromatase R264C (lane 4). GAPDH was used as a control of equal loading or transfer. C) Specific activity of aromatase in MOCK ST14A neuronal cells or cells transiently transfected with full-length aromatase WT, full-length aromatase R264H and full-length aromatase R264C. Data points are the average of four independent measurements and error bars represent the standard deviation. D) Western blot analysis performed on 15 µg total cellular proteins extracted from MOCK ST14A cells (lane 1), full-length aromatase WT- (lane 2), full-length aromatase R624H- (lane 3) and full-length aromatase R264C- (lane 4) transfected cells. GAPDH was used as as a control of equal loading or transfer.

Tables

Table 1. Melting temperatures (T_m) and kinetic parameters ($\mathbf{K_M}$ and $\mathbf{k_{cat}}$) calculated for rArom WT, rArom R264H and rArom R264C.

rArom variant	T_m **(°C)**		**K_D (µM)**	**K_M (µM)**	**k_{cat} (min^{-1})**	**Catalytic efficiency (k_{cat}/K_M)**
	Ligand-free	**Androstenedione-bound**				
WT	52.9 ± 0.3 [33]	55.7 ± 0.3 [33]	1.2 ± 0.1 [33]	0.46 ± 0.06	1.9 ± 0.1	4.1
R264H	48.0 ± 0.3 **	52.5 ± 0.2 **	2.3 ± 0.1**	1.14 ± 0.10**	1.4 ± 0.1**	1.2
R264C	49.8 ± 0.2**	53.0 ± 0.3**	2.3 ± 0.1**	0.74 ± 0.07 *	2.1 ± 0.1	2.8

Table 2. rArom WT, R264H and R264C residual activity (%) upon phosphorylation and treatment with kinases inhibitors.

	rArom activity (%)				
rArom variant	**Controls**	**+ 40 ng PKA**	**+ 40 ng PKA + 10 µM H89**	**+ 100 ng PKG1**	**+ 100 ng PKG1 - cGMP**
WT	100 ± 3.5	63.8 ± 2.1 **	89.9 ± 2.1	69.7 ± 7.7 *	98.6 ± 2.0
R264H	100 ± 2.1	72.1 ± 4.3 **	95.4 ± 4.3	84.6 ± 4.7 *$^{\#}$	97.1 ± 2.1
R264C	100 ± 2.0	50.7 ± 2.0 **$^{\#\#}$	92.3 ± 2.1	69.5 ± 5.5 *	95.8 ± 3.9

P-value < 0.05 by one-way ANOVA and ** P-value < 0.001 by one-way ANOVA refer to samples treated with kinases rArom compared to controls. $^{\#}$ P-value < 0.05 by one-way ANOVA and $^{\#\#}$ P-value < 0.001 by one-way ANOVA refer to the polymorphic variants treated with kinases compared to rArom WT treated with kinases.

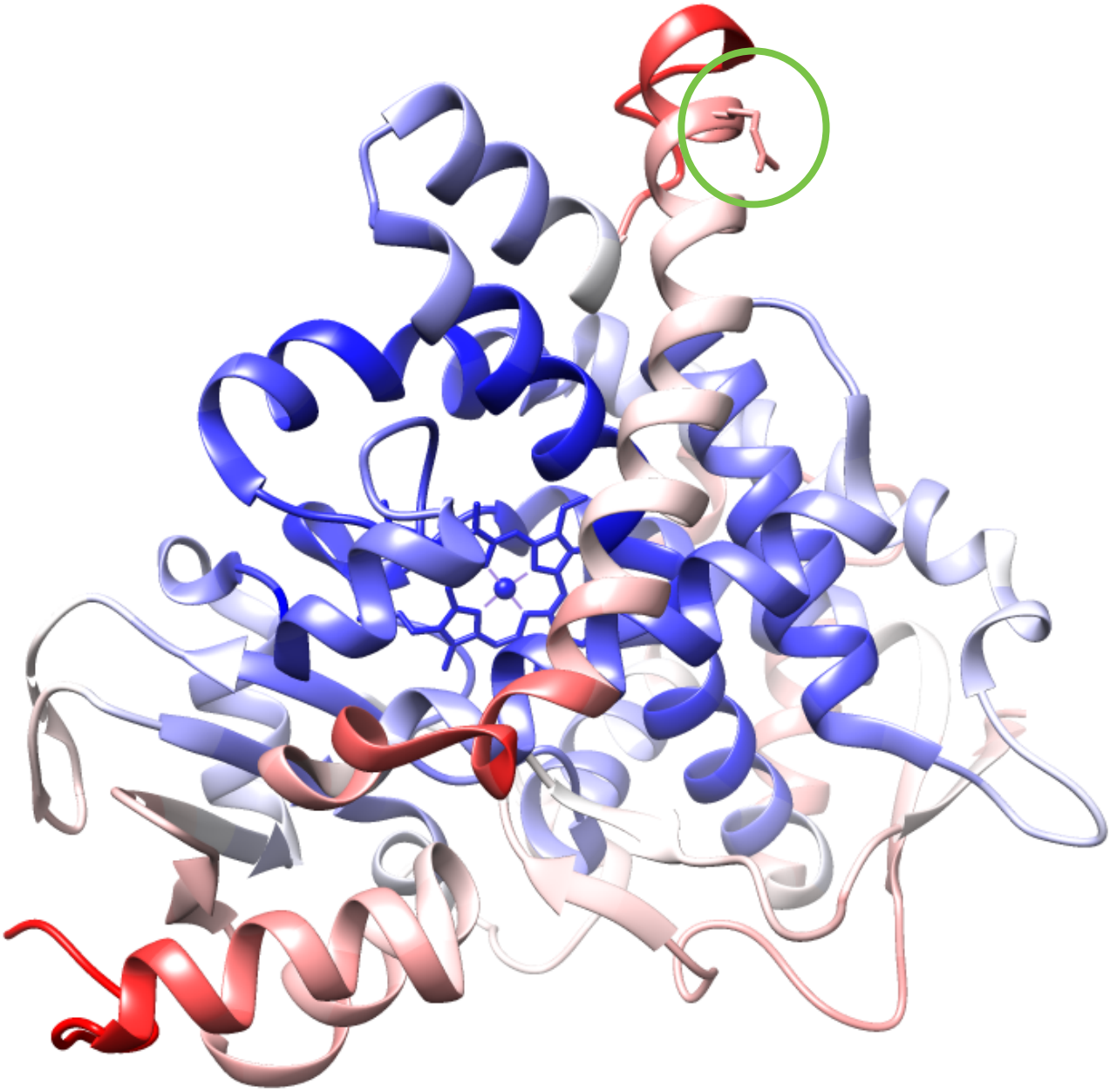

Figure 1

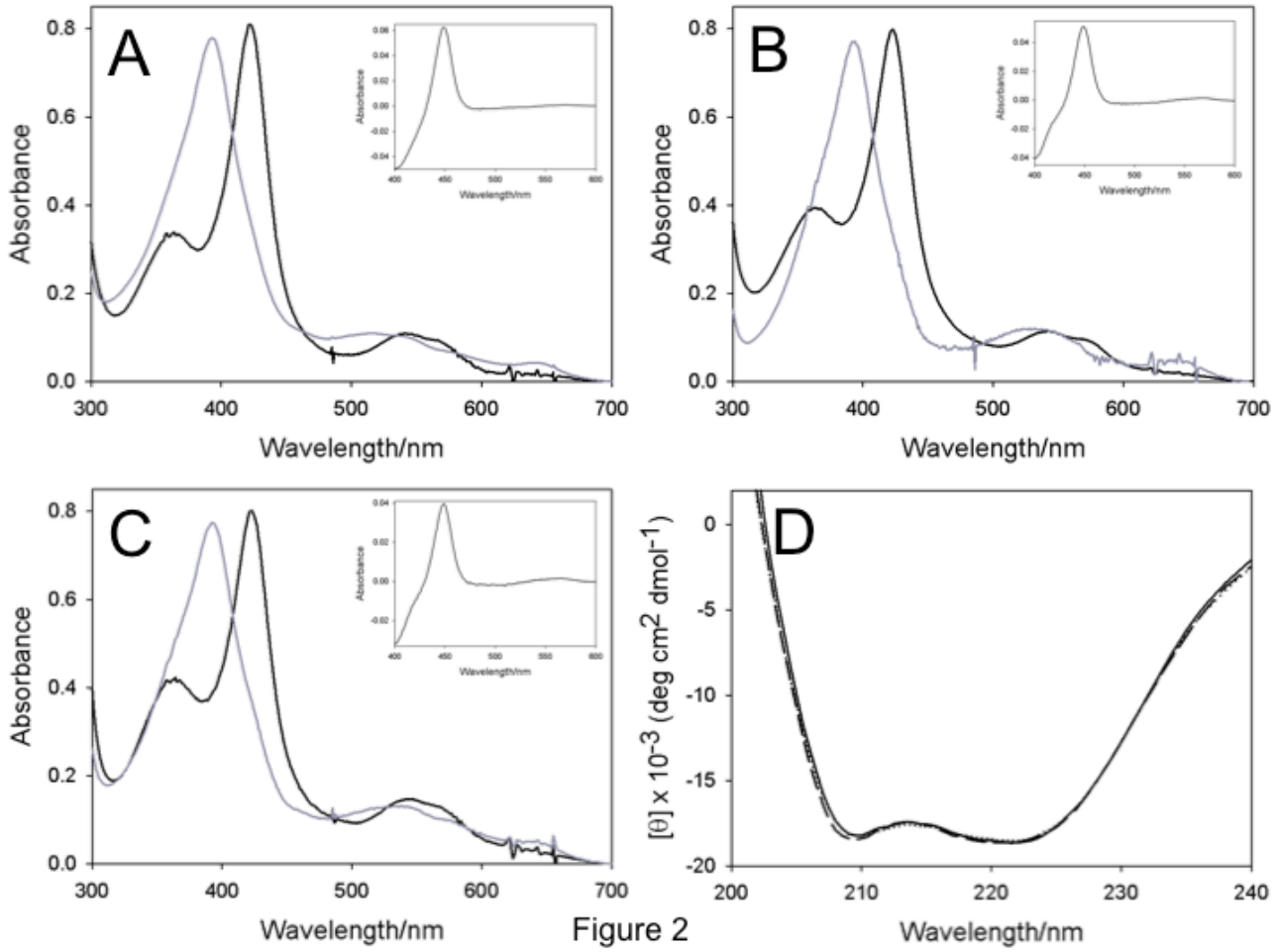

Figure 2

A

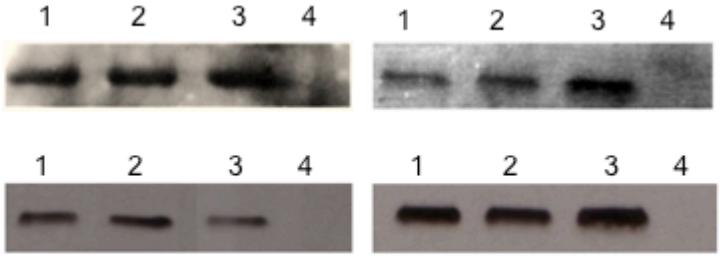
1 2 3 4
1 2 3 4
1 2 3 4
1 2 3 4

B

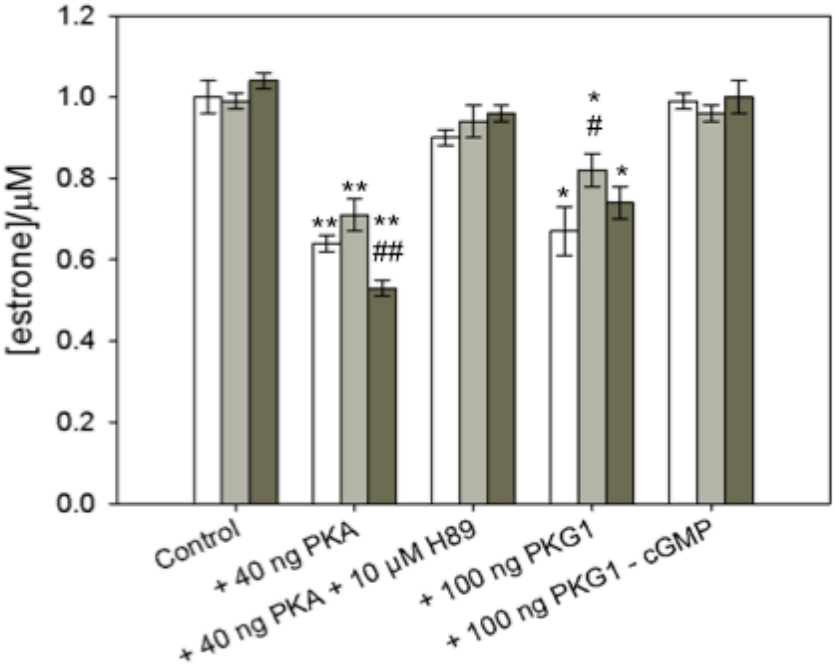
[estrone]/µM
1.2
1.0
0.8
0.6
0.4
0.2
0.0
**
**
**
##
*
#
*
*
Control
+ 40 ng PKA
+ 40 ng PKA + 10 µM H89
+ 100 ng PKG1
+ 100 ng PKG1 - cGMP

Figure 3

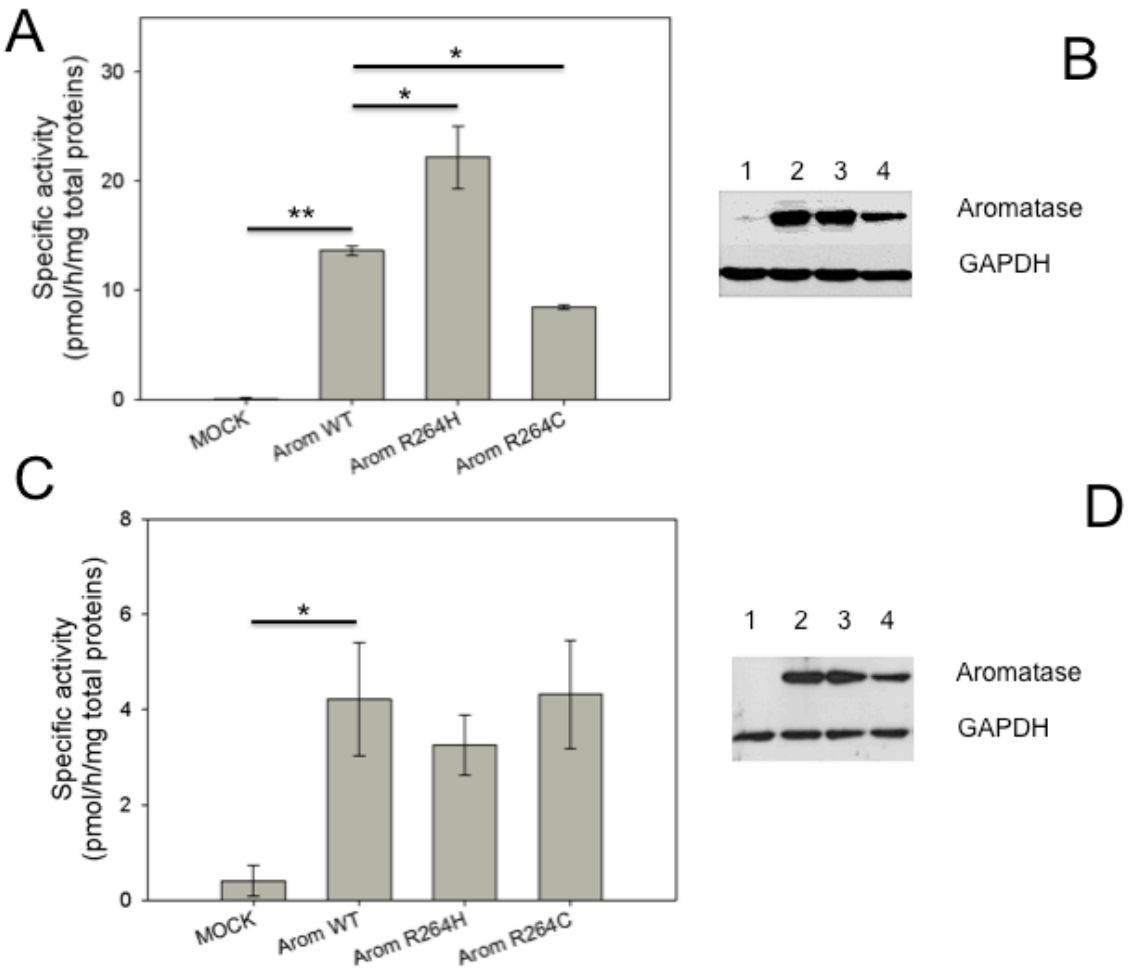
A
B
C
D
Specific activity
(pmol/h/mg total proteins)
0
10
20
30
*
*
**
MOCK
Arom WT
Arom R264H
Arom R264C
1 2 3 4
Aromatase
GAPDH
0
2
4
6
8
*

Figure 4